POLITECNICO DI TORINO
Repository ISTITUZIONALE

Diagnosis of Faulty Wind Turbine Bearings Using Tower Vibration Measurements

Original
Diagnosis of Faulty Wind Turbine Bearings Using Tower Vibration Measurements / Castellani, F., Garibaldi, L., Daga, A.P., Astolfi, D., Natili, F.. - In: ENERGIES. - ISSN 1996-1073. - 13:6(2020), p. 1474. [10.3390/en13061474]

Availability:
This version is available at: 11583/2805174 since: 2020-03-23T10:03:53Z

Publisher:
MDPI

Published
DOI:10.3390/en13061474

Terms of use:

This article is made available under terms and conditions as specified in the corresponding bibliographic description in the repository

Publisher copyright

(Article begins on next page)

18 November 2026

energies

MDPI

Article

Diagnosis of Faulty Wind Turbine Bearings Using Tower Vibration Measurements †

Francesco Castellani [1], Luigi Garibaldi [2], Alessandro Paolo Daga [2], Davide Astolfi [1,*] and Francesco Natili [1]

[1] Department of Engineering, University of Perugia, Via G. Duranti 93, 06125 Perugia, Italy; francesco.castellani@unipg.it (F.C.); francesco.natili@studenti.unipg.it (F.N.)

[2] Department of Mechanical and Aerospace Engineering, Politecnico di Torino, Corso Duca degli Abruzzi 24, 10129 Torino, Italy; luigi.garibaldi@polito.it (L.G.); alessandro.daga@polito.it (A.P.D.)

* Correspondence: davide.astolfi@unipg.it; Tel.: +39-075-585-3709

† This paper is an extended version of our paper published in Surveillance, Vibrations, Shocks and Noise (SURVISHNO 2019), Lyon, France, 8–10 July 2019.

Received: 30 January 2020; Accepted: 17 March 2020; Published: 20 March 2020



Abstract: Condition monitoring of gear-based mechanical systems in non-stationary operation conditions is in general very challenging. This issue is particularly important for wind energy technology because most of the modern wind turbines are geared and gearbox damages account for at least the 20% of their unavailability time. In this work, a new method for the diagnosis of drive-train bearings damages is proposed: the general idea is that vibrations are measured at the tower instead of at the gearbox. This implies that measurements can be performed without impacting the wind turbine operation. The test case considered in this work is a wind farm owned by the Renvico company, featuring six wind turbines with 2 MW of rated power each. A measurement campaign has been conducted in winter 2019 and vibration measurements have been acquired at five wind turbines in the farm. The rationale for this choice is that, when the measurements have been acquired, three wind turbines were healthy, one wind turbine had recently recovered from a planetary bearing fault, and one wind turbine was undergoing a high speed shaft bearing fault. The healthy wind turbines are selected as references and the damaged and recovered are selected as targets: vibration measurements are processed through a multivariate Novelty Detection algorithm in the feature space, with the objective of distinguishing the target wind turbines with respect to the reference ones. The application of this algorithm is justified by univariate statistical tests on the selected time-domain features and by a visual inspection of the data set via Principal Component Analysis. Finally, a novelty index based on the Mahalanobis distance is used to detect the anomalous conditions at the damaged wind turbine. The main result of the study is that the statistical novelty of the damaged wind turbine data set arises clearly, and this supports that the proposed measurement and processing methods are promising for wind turbine condition monitoring.

Keywords: wind energy; wind turbines; condition monitoring; vibration analysis; signal processing

1. Introduction

The diagnosis of gears and bearings faults of gearbox systems [1] is particularly challenging, especially if the machine of interest is subjected to non-stationary operation conditions.

Most of the wind turbines currently operating for industrial uses have a three-stage gearbox for transforming the rotation of the blades (order of 10 revolutions per minute) into the generator rotational speed. There are several studies about wind turbine reliability [2,3] and down-time rates [4], and it is estimated [5] that at least 20% of the non-availability time of a wind turbine is caused by a

gearbox failure. Therefore, the development of effective gearbox condition monitoring techniques is a keystone for the optimization of wind turbine availability and for the energy cost minimization.

Nevertheless, the elaboration and interpretation of drive-train vibration measurements are complex and this matter of fact produces an under-exploitation of this kind of data in the wind energy practitioners community. Oil particle counting [6] and operation data analysis (especially temperatures, as, for example, in [7–11]) are widely used techniques for condition monitoring: they are more easily interpretable, but the drawback is that they furnish a later stage and more uncertain fault diagnosis, with respect to sub-component vibration spectra analysis. This remark is supported quantitatively in the work [12], where large amounts of labeled wind turbine supervisory control and data acquisition (SCADA) and vibration data have been processed, and the conclusion is that operation data can be used for reliably diagnosing a failure approximately one month before it occurs, while high frequency vibration data can be used to extend the accurate prediction capability to five to six months before failure. Furthermore, using operation data analysis, the fault diagnosis can successfully be performed through Artificial Intelligence techniques approximately 75% of the time, while, using vibration data, this percentage rises to 100%.

On these grounds, it is particularly valuable to develop vibration measurement and analysis techniques that can reliably spread in the wind energy industry practice, and the present study aims at providing a contribution to this objective.

The literature about vibration analysis for wind turbine condition monitoring has been particularly developing in the latest years: for example, in [13], data mining algorithms and statistical methods are used for interpreting vibration measurements collected at wind turbine gearbox in the time and frequency domains. In [14], three techniques are proposed for wind turbine gearbox condition monitoring in the time-domain: signal correlation, extreme vibration, and Root Mean Square (RMS) intensity. RMS and extreme values

result in being particularly meaningful damage indicators.

The work in [15] deals with condition monitoring of wind turbine drive-train bearings, and an important challenge is successfully tackled: the separation of the faulty bearing signatures from the masking signals, due to the other rolling elements like the gears or the shafts. This can be obtained on the basis of the fact that the signatures due to gears and shafts are deterministic and bearing signatures are stochastic and can be treated as cyclo-stationary [16] around their fundamental period. In [17], a simplified nonlinear gear model is at first developed, on which a time–frequency method is applied for a first overview; subsequently, the case of varying loads is examined through Empirical Mode Decomposition (EMD), for decomposing the vibration signals into meaningful components associated with specific frequency bands. The EMD is employed also in [18], where an enhanced Empirical Wavelet Transform method is proposed and tested on open access data of wind turbine gears and bearings: the results support that the proposed method is effective for segmenting the frequency spectrum of the signal and for detecting the fault-related features. In [19], a critical analysis of the synchrosqueezing transform for the representation of non-stationary signals is proposed: for this aim, the synchrosqueezing transform is improved using iterative generalized demodulation and the proposed method is validated using both numerically simulated and experimental vibration signals of wind turbines planetary gearboxes. Finally, for comprehensive and recent reviews about wind turbine drive-train condition monitoring techniques, refer to [12,20,21].

Basing on the above literature discussion, it can be fairly stated that many powerful techniques for the analysis of wind turbine vibration signatures are based on cyclo-stationarity. The downside is that this kind of analysis is particularly demanding as regards the data because, for example, the angular speed must be measured at high sampling rates, and this is not guaranteed even by using time-resolved operation data (as, for example, the ones analyzed in [22,23]): for this reason, most of the studies deal with numerical simulations [19] and laboratory test rig measurements [24]. On the other side, it should be noticed that industrial wind turbines are commonly equipped with commercial

condition monitoring systems: these do not stock measurements continuously (they record when some trigger events occur) and stock them in treated form instead of raw.

As regards the circumvention of the above limitations, one remarkable study is [25]: it resulted in being inspiring for the purposes of the present work because it dealt with wind turbine generators' condition monitoring through the analysis of sound and vibration measured at the tower. Empirical Mode Decomposition (EMD) is employed for processing the measurements and the results of this analysis are put in relation with the vibrations collected directly at the sub-component of interest. The conclusion of [25] is that tower vibrations contain intelligible signatures of the generator bearing damage. Other inspiring studies for the purposes of the present work are [26–28] because dealing with the analysis of very extremely modulated real-world wind turbine gearboxes data. The study in [28] deals with vibration data sets provided by Suzlon, and it shows that the Signal Intensity Estimator (SIE) offers a good overall picture of time-frequency space by which a broken gear tooth could simply be identified. Data-inspection techniques similar to the ones of this work are adopted, as, for example, the Principal Component Analysis on a set of statistical features computed from the vibration data. The use of Signal Intensity Estimator as a time-frequency fault indicator has been explored and supported also in [26]: the selected test case is a bearing outer race fault at a Repower wind turbine. The case has been selected because it has been considered very representative of scenarios where factors such as structural noise and variation in speed and load lead to different modulation rates of the vibration signals. The use of Signal Intensity Estimator for bearing damage detection is discussed as well in [27], where comparisons are carried against commonly employed statistical indicators like kurtosis and crest factor.

On these grounds, the present study is devoted to the analysis and post-processing of tower vibrations for condition monitoring of drive-train bearings of horizontal-axis wind turbines. A qualifying point of this work is that it is based on a particularly valuable real test-case discussion. Measurements have been collected at a wind farm sited in Italy, owned by Renvico (a company managing around 340 MW of wind turbines in Italy and France, www.renvicoenergy.com), featuring six 2 MW wind turbines. Five wind turbines have been selected for this study: three reference healthy ones and two target ones. The former target wind turbine is damaged at the high-speed shaft bearing, the latter target wind turbine had a planetary shaft bearing damage, and the bearing of interest was substituted some weeks before the measurement campaign was conducted. Therefore, the two target wind turbines are a damaged and a recovered one. The non-stationary conditions to which wind turbines are subjected are taken into account in the proposed methods by aggregating measurements acquired simultaneously at the highest possible number of wind turbines under the assumption they are subjected to the same wind field (which is not true, but commonly acceptable). Given the limited number of available instrumentation (i.e., two acquisition systems), it has been assumed acceptable also to compare nearly-simultaneous time series (i.e., collected consecutively, order of some minutes) because the variation of the wind field on such a time scale does not affect the robustness of the measurement processing algorithm.

If the methods proposed in this work are reliable, it should be possible to distinguish the damaged target wind turbine with respect to the reference healthy ones, while the recovered wind turbine should be indistinguishable with respect to the reference ones. In this work, it is shown that this is indeed the case. In summary, the post-processing algorithm proceeds as follows: vibration measurements are analyzed through a multivariate Novelty Detection algorithm in the feature space, whose reliability is supported by univariate analysis of variance on the selected time-domain features and by Principal Component Analysis. Finally, a novelty index based on the Mahalanobis distance is used to distinguish the target from the reference wind turbines.

The results collected in this work support that the proposed measurement and post-processing methods are reliable for effective condition monitoring of wind turbine drive-train bearings. it should be noticed that an important point of strength of this work is the fact that measurements are collected at the tower, without intervening in the normal operation of the wind turbines of interest. This is a

remarkable aspect about the generalization and repeatability of the proposed methods and it deals as well with open access ideology because it allows circumventing, with a relatively low cost, the fact that raw vibration data from commercial condition monitoring systems are typically at the disposal of only of wind farm manufacturers, thus excluding wind farm owners and managers and scholars.

The structure of the manuscript is the following: in Section 2, the test case, the measurements, and the collected data sets are introduced. Section 3 is devoted to the methodology description, while the results are collected and discussed in Section 4. Finally, conclusions are drawn in Section 5.

2. The Test-Case and the On-Site Measurements

The wind farm is comprised of six multi-MW wind turbines, and it is located in southern Italy. The layout of the wind farm is reported in Figure 1: the lowest inter-turbine distance on site is on the order of seven rotor diameters. The damaged wind turbine (WTG03) is indicated in red, the healthy reference wind turbines (WTG02, WTG04, WTG05) are indicated in green, and the recovered wind turbine (WTG06) is indicated in blue. The damage at WTG03 regards the high speed shaft bearing, and the recovered damage at WTG06 is regarded as a planetary bearing. The damage at WTG03 has been independently diagnosed on the basis of oil particle counting; the severity of the damage was not high enough to request wind turbine stop (otherwise, the present analysis would not have been possible). In order to provide a qualitative indication of the damage severity, consider that the bearing of interest has been replaced three and a half months after the measurement campaign of this work was conducted.

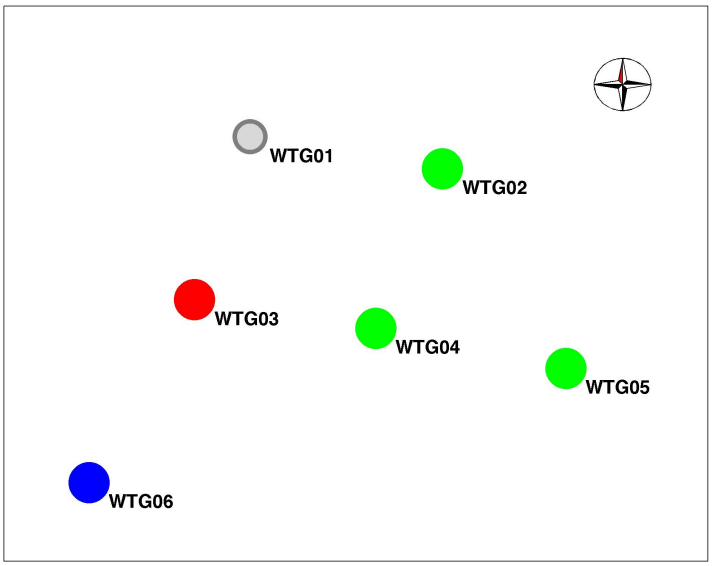


Figure 1. The layout of the wind farm. The healthy wind turbines are indicated in green, the damaged in red, and the recovered in blue.

The measurement procedure is the following: accelerometers have been employed inside the tower of the wind turbine, measuring the longitudinal (x-axis) and transversal (y-axis) vibrations at a height of the order of two meters with respect to the tower base. A sketch is reported in Figure 2. Each acquisition therefore consists of two channels, and these are sampled at 12.8 kHz for at least 2 min.

The wind turbine owner and the wind turbine manufacturer have provided in real time operation data having a sampling time of the order of the second. These have been used to verify that the wind turbines were undergoing reasonably similar conditions and were operating in a reasonably similar way. It has been observed that this was the case. Despite the fact that the reliability of the method is not considered to depend on the particular conditions on site, as long as these conditions are similar

for all the measurement acquisitions; for completeness sake, it is reported that, during the acquisitions of Table 1, the prevailing wind intensity and direction were respectively 7 m/s and 330° for all the wind turbines. The average produced power was on the order of 30% of the rated. An interesting observation regards the fact that the measurements employed in this study have been collected at a low-moderate wind intensity; commercial condition monitoring techniques—instead, trigger and stock data at the disposal only at rated power.

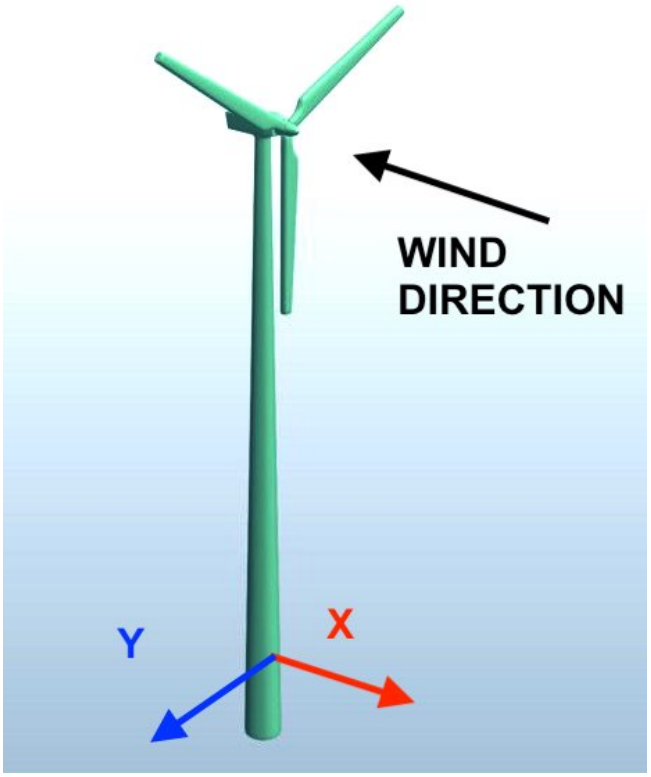


Figure 2. Definition of the reference frame for the longitudinal and the transversal directions.

Table 1. The time series selection.

TS Number	Wind Turbine	Wind Turbine Status	Acquisition Time	Use	Generator rpm
1	WTG02	healthy	14:15	reference - calibration	1362
2	WTG04	healthy	14:55	reference - calibration	1199
3	WTG05	healthy	15:25	reference - calibration	1185
4	WTG02	healthy	14:25	reference - validation	1242
5	WTG04	healthy	15:05	reference - validation	1376
6	WTG05	healthy	15:35	reference - validation	1083
7	WTG06	repaired	13:00	target - validation	1694
8	WTG06	repaired	13:10	target - validation	1584
9	WTG06	repaired	13:20	target - validation	1537
10	WTG03	damaged	13:00	target - validation	1585
11	WTG03	damaged	13:10	target - validation	1468
12	WTG03	damaged	13:20	target - validation	1579
13	WTG03	damaged	14:15	target - validation	1338
14	WTG03	damaged	14:25	target - validation	1399
15	WTG03	damaged	14:55	target - validation	1333
16	WTG03	damaged	15:05	target - validation	1365
17	WTG03	damaged	15:25	target - validation	1274
18	WTG03	damaged	15:35	target - validation	1207

The vibration time series have been organized as indicated in Table 1, with a progressive numbering of the time series. The time series have been labeled for future reference in the following

methods and analysis. The results reported in the following refer to this particular time series arrangement, but it should be noticed that crosschecks have been performed by interchanging TS1–6 and by selecting an arbitrary subset of TS1–6 for the training and the substance, as expected, is unchanged. The rationale for these crosschecks is supporting the fact that the proposed method does not highlight as novelty wind turbines undergoing slightly different operation conditions (because the wind field has varied in time and-or space), but it highlights, as shall be shown in Sections 3 and 4, the statistical novelty of faulty wind turbines.

It is important to notice that acquisitions have been performed within 3 h, but there are always two contemporary acquisitions (one at reference wind turbines and one at the targets), so that the risk that operational or environmental effects could be confounded for damage is reduced.

3. Methods

Due to the complexity of the windmills structures and of the possible acquisition disturbances in the measurement chain, the on-site accelerometric measurements are usually very noisy. In this particular case, many acquisitions show unphysical trends that must be removed. Nevertheless, additional anomalies could be found, which are induced by the natural variability of the wind. Changes in wind direction or intensity affect the work condition of the machine, which is usually adapted to the condition by rotating the whole nacelle upwind (i.e., with the rotor facing the wind) and by controlling the pitch angle of the blades so as to obtain the maximum generated power without exceeding the maximum rotational speed.

According to these considerations, before the feature extraction step, a data pre-processing needs to be implemented to clean the acquisitions so as to remove confounding influences that could be detrimental for the diagnostics via anomaly detection. The data pre-processing proposed in this work is described in Sections 3.1–3.3, and consists of three steps:

1. a pre-treatment of the single accelerometric tracks to remove the unphysical trends;
2. the extraction of the selected features;
3. a multivariate cleaning to recognize and remove from the analysis the chunks of the signal where the machine is in adaptation to a change of the work condition.

Finally, in Section 3.4, the statistical data processing, implemented to analyze the dataset and performing the damage detection, is described. The investigation is divided in three sub-analyses:

1. At first, the goodness of the selected features and of the pre-processing is assessed univariately. This is performed as a univariate test of hypothesis exploiting the ANOVA to investigate the damage detection ability of the single features extracted from the two different channels.
2. Then, in order to visualize the multivariate dataset, a PCA is performed.
3. Finally, an unsupervised damage detection implemented in terms of multivariate Novelty Detection is used to detect the damaged windmill that stands out from the other machines.

A scheme of the work flow is reported in Figure 3.

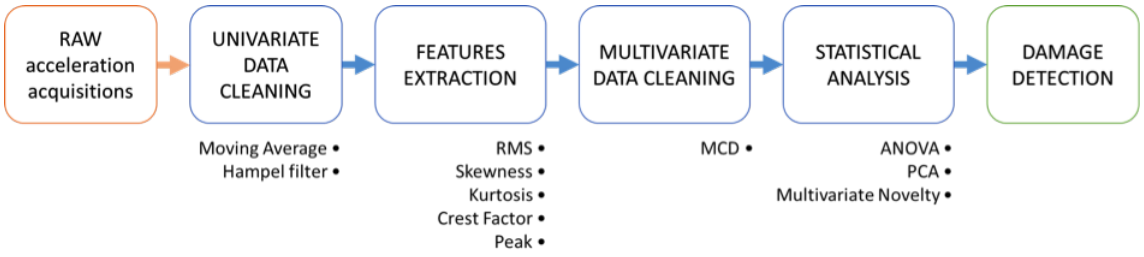


Figure 3. Block diagram of the data analysis procedure.

3.1. Univariate Data Pre-Processing

The available acceleration signals feature acquisition anomalies, probably due to the strong electromagnetic fields that can interest the area around the windmills. In particular, non-physical trends appear in the measured accelerations. To overcome this issue, a data cleaning is proposed in this paper to pre-process the data before any further analysis: in Figures 4 and 5, the raw and post-processed data are shown.

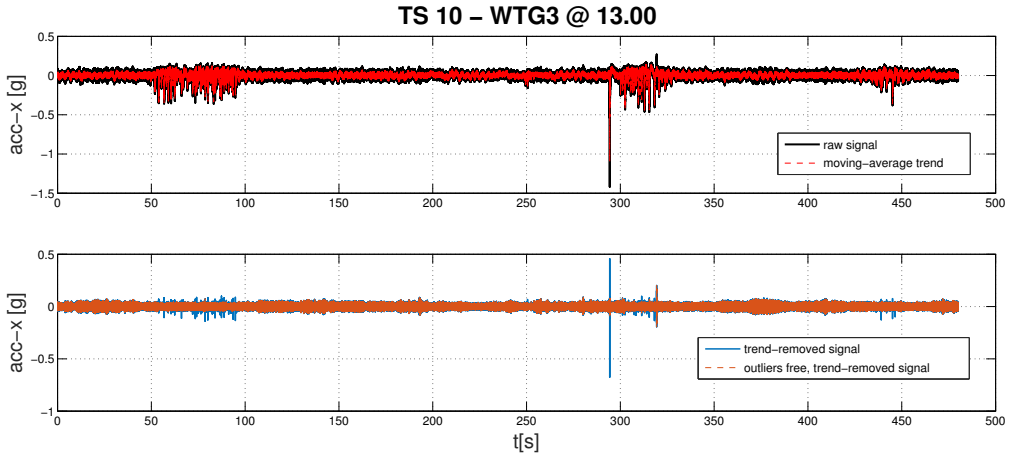


Figure 4. A sample time series of the raw and processed signal.

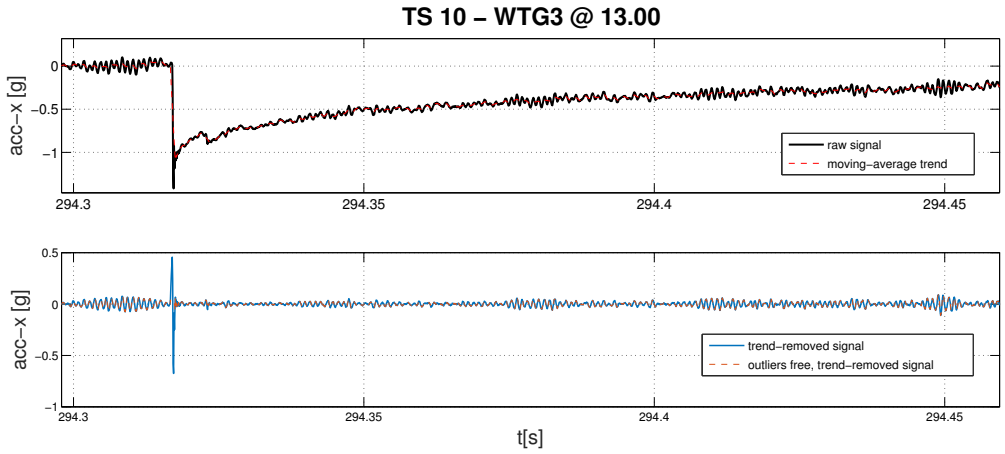


Figure 5. Zoom on a sample time series of the raw and processed signal.

In signal processing, it is very common to deal with trends by considering them as the low-frequency content of the signal, which can be then divided into a long-term contribution (i.e., the trend), and a short-term (high frequency) contribution. Hence, a trend can be highlighted by low-pass filtering the original signal to remove the high-frequency fluctuations. Many kinds of digital low-pass filters are present in the literature, as well as plenty of filter design criteria. Nevertheless, the simplest yet causal (i.e., which uses only past values to compute the present output, and is then suitable for online implementation) digital filter is without any doubt the moving average filter, which is also the optimal filter for reducing random noise while retaining a sharp step response [29]. The moving average filter (sometimes defined as "boxcar filter" because of the rectangular shape of its corresponding weighting window) can be defined through its impulse response (Equation (1)):

$$h[n] = \begin{cases} \frac{1}{M}, & 0 \leq n < M \\ 0, & n < 0 \vee n \geq M \end{cases} \quad (1)$$

and applied via convolution (Equation (2)) on the raw signal $s[n]$:

$$s_f[n] = s[n] \cdot h[n] = \sum_{m=-\infty}^{\infty} s[m]h[n-m]. \tag{2}$$

An approximate half power cut-off frequency of such a filter can be found starting from the frequency response of an M point moving average filter (Equations (3) and Figure 6):

$$|H(\omega)| = \frac{1}{M}\left|\frac{\sin\left(\frac{\omega M}{2}\right)}{\sin\left(\frac{\omega}{2}\right)}\right| = \frac{1}{M}\left|\frac{\sin\left(\frac{\pi M f}{f_s}\right)}{\sin\left(\frac{\pi f}{f_s}\right)}\right|, \tag{3}$$

where f_s is the sampling frequency of the signal.

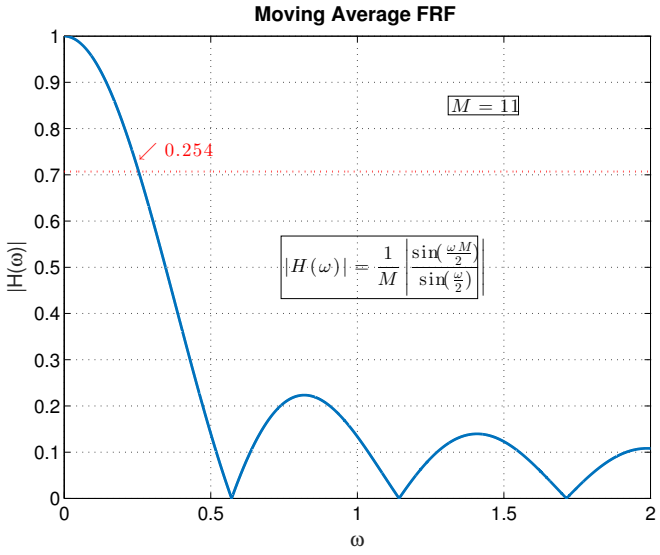


Figure 6. Example of frequency response of a moving average filter.

With $M = 11$, a cut-off of roughly $f_{co} = 0.254\frac{f_s}{2\pi} \simeq 500$Hz is obtained, which proved to be appropriate for the case under analysis.

The so estimated trend has been removed from the raw data by subtraction, and this can be appreciated by comparing the upper subplots in Figures 4 and 5, respectively, for the whole signal and for a sample chunk of it. Furthermore, some abnormal spikes can still be found in the residual signal. In order to compensate also for this effect, a Hampel filter is used. The Hampel filter is an online two-step procedure meant to identify univariate outliers in a short window of the signal (i.e., local outliers) and substitute such samples with more plausible values. To ensure robustness, the local outliers are not identified through the usual 3σ rule (i.e., a value which is farther than three times the standard deviation σ from the mean value μ is considered an outlier at a confidence of 99.7%), but using the median and the median absolute deviation MAD [30,31]. If a sample from the windowed signal s_w (i.e., a chunk of the signal in the $\pm MM$ samples range) falls out of the confidence interval of

$$|s_w - median(s_w)| \leq 3 \cdot 1.4826 MAD \tag{4}$$

it is considered an outlier and is removed and substituted with the median value median(s_w). In this work, a window of $MM = \pm 22$ samples was used, as this window size proved to lead to good results in all the acquisitions. The result of this outlier removal on a sample signal (previously de-trended) is depicted in the lower subplots of Figures 4 and 5.

3.2. Features Extraction

The information regarding the state of health of the wind turbine must be extracted from the vibration data. The first step is selecting meaningful damage-distinguishing characteristics (commonly called features) for extracting information on the damage. The feature selection is a critical point: in fact, the ideal feature is sensitive to incipient damage but is not influenced by environmental or operational variability. For a geared machine operating in non-stationary conditions, as a wind turbine is, spectral lines are particularly sensitive to damages: as argued in Section 1, the main points as regards spectrum analysis are enhancing the signal-to-noise ratio and taking into account non-stationary conditions. Furthermore, for geared systems, it is necessary to know the geometry of the gearbox in order to identify the gear-mesh frequencies. For these reasons, it is not a priori guaranteed that all the necessary information is available for an effective spectral analysis for a case study as the one in the present work; furthermore, in any case, it is likely that considerable human supervision is needed in the feature extraction process. Some techniques for damage detection based on lower-level features, on the contrary, can avoid human supervision and can outperform the spectral features in terms of repeatability and reliability. This approach will be employed in the following: it is based on the idea that the modification in the probability distribution of the measured acceleration y is due to a malfunctioning. The acceleration y is a discrete variable because it is measured with a given sampling frequency. For this reason, in the following, it is labeled as $y(k)$ and its standard deviation is labeled as σ_y.

On the grounds of the above reasoning, for this work, the following features have been selected:

- Root Mean Square: it represents not only the width of the probability density function of y, but also the average power of a stationary process, and it is a robust measure of the acceleration level. It is defined as
$$RMS = \sqrt{E\left[y(k)^2\right]} \tag{5}$$
- Skewness: it is a measure of the symmetry of a probability distribution. it is defined as
$$SKEW = E\left[\left(\frac{y(k)}{\sigma_y}\right)^3\right] \tag{6}$$
- Kurtosis: it is a measure of tailedness of the probability distribution and therefore it quantifies the importance of the tail extremity and is sensitive to outliers. It is defined as
$$KURT = E\left[\left(\frac{y(k)}{\sigma_y}\right)^4\right] \tag{7}$$
- Peak: it is defined as
$$PEAK = max(abs(y(k)) \tag{8}$$
- Crest factor: it is defined as the ratio between peak value and root mean square. it is employed for anomaly detection because of its responsiveness to impulse.
$$CREST = \frac{PEAK}{RMS} \tag{9}$$

The above definitions are under the assumption that the acceleration signal y has vanishing mean.

To guarantee the reliability of the method, many measurement points are necessary [32,33]. The above features have therefore been extracted on independent (no overlap) chunks of the original signals: each acquisition is divided in 100 sub-parts which the five features are computed. Doing this, one obtains a features matrix X where the number of columns is $n = 10$ and it is given by the product of the number of channels (2) times the number of computed features (5); the number of rows

is $d = 1800$ and it corresponds to number of chunks extracted from the 18 acquisitions of Table 1 placed consecutively.

3.3. Multivariate Data Cleaning

The stochastic variability of the wind strongly affects the work condition of the machine, which adapts to wind direction and intensity, inducing anomalies in the acquired signal. Such anomalies are often so important that can be easily noticed by eye; nevertheless, in order to automate the analysis, a routine is here proposed for removing the data-points in the 10-dimensional ($d = 10$) feature space (five features, two channels), which are multivariate outliers with respect to the sample of 100 observations corresponding to the particular acquisition (each channel was divided in 100 independent chunks on which the five features were computed).

In multivariate statistics, the detection of outliers is usually tackled using a 3σ equivalent rule, which in the multidimensional space translates into a 99,7% tolerance ellipsoid rule. This can be easily implemented through the Mahalanobis distance, which corresponds to the standardized distance of a point from the centroid ($\bar{X}$) of the ellipsoid defined by the covariance matrix $\boldsymbol{S} = \frac{1}{N}(\boldsymbol{X} - \bar{\boldsymbol{X}})(\boldsymbol{X} - \bar{\boldsymbol{X}})^T$ the Mahalanobis distance MD is defined as (Equation (10)):

$$MD = \sqrt{(\boldsymbol{X} - \bar{\boldsymbol{X}})\,\boldsymbol{S}^{-1}\,(\boldsymbol{X} - \bar{\boldsymbol{X}})}, \tag{10}$$

so that, if the estimates $\bar{\boldsymbol{X}}$ and $\boldsymbol{S}$ can be confused with the true values and $\boldsymbol{X}$ is assumed normal, the simple confidence interval based on the chi-squared (χ^2) critical value holds (Equation 11):

$$MD < \sqrt{\chi^2_{d;0.997}}. \tag{11}$$

Similarly to what happens in the univariate case, if the number of samples is not high enough to ensure reliable estimates, or if outliers are present distorting such estimates, the assumption of a χ^2 distribution for the MD does not hold anymore. Nevertheless, this can be fixed if a robust estimation of $\bar{\boldsymbol{X}}$ and $\boldsymbol{S}$ is performed. A simple but effective method for getting robust estimates of $\bar{\boldsymbol{X}}$ and $\boldsymbol{S}$ is thorough the Minimum Covariance Determinant (MCD) [34]. Briefly, MCD is an iterative procedure to select the h observations out of N (where $N/2 < h \leq N$) whose classical covariance matrix has the lowest possible determinant. The ratio h/N is called Outlier Fraction, and is the only parameter affecting the algorithm, which will be used in this work in its Fast implementation. Using such a routine, a Robust Mahalanobis distance RD can be obtained so that the confidence interval in Equation (12):

$$RD = \sqrt{(\boldsymbol{X} - \bar{\boldsymbol{X}}_{MCD})\,\boldsymbol{S}^{-1}_{MCD}\,(\boldsymbol{X} - \bar{\boldsymbol{X}}_{MCD})} < \sqrt{\chi^2_{d;0.997}} \tag{12}$$

can be used to test for outliers. In this work, this method is used to remove the multivariate outliers independently from each of the 100 sample subsets corresponding to the different acquisitions, so as to clean out the data associated with machine adaptation to wind. Using an outlier fraction of 10%, 1520 samples are left, starting from the original 1800 observations.

3.4. Statistical Analysis

3.4.1. Hypothesis Test

A statistical hypothesis test is a method of statistical inference for comparing two statistical samples, or a sample against a model. A hypothesis is proposed for the statistical relationship among the two, and this is compared to an alternative suggesting no relationship. The comparison is considered statistically significant if the relationship is estimated as an extremely unlikely realization of the null hypothesis according to a threshold probability. The p-value is the probability that, assuming the null hypothesis H_0, the statistical summary is more extreme than the actual observed results.

Hence, if the obtained p-value is less than or equal to a selected significance level α, the null hypothesis is rejected. A typical value of α is 0.05 (5%).

The ANOVA (univariate Analysis of Variance) is a statistical method to test, basing on the variance analysis, the null hypothesis H_0 that all the considered groups populations come from the same distribution: in other words, the null hypothesis corresponds to the fact that no significant difference is detectable among the groups. The null hypothesis will be accepted or rejected according to a statistical summary $\hat{F}$ which, under the assumptions of independence, normality and homoscedasticity of the original data, follows a Fisher distribution:

$$\hat{F} = \frac{\frac{\sigma_{bg}^2}{G-1}}{\frac{\sigma_{wg}^2}{N-G}} \simeq F(G-1, N-G), \tag{13}$$

where

$$\sigma_{bg}^2 = \sum_{j=1}^{G} \frac{n_j}{N} \left(\bar{y} - \mu_j\right)^2, \tag{14}$$

$$\sigma_{wg}^2 = \frac{1}{N} \sum_{j=1}^{G} \sum_{i=1}^{n_j} \left(\bar{y}_{ij} - \mu_j\right)^2, \tag{15}$$

with G being the number of groups of size n_j, N being the global number of samples with overall average $\bar{y}$, σ_{bg}^2 being the variance between the groups, σ_{wg}^2 being the variance within the groups (basically the average of the variance computed in each group) [35]. The null hypothesis H_0 will be accepted with a confidence level $1-\alpha$ if the summary $\hat{F}$ is less extreme than a critical value $F^{\alpha}(G-1, N-G)$. The corresponding p-value is computed: it represents the the probability that the summary is more extreme than the observed $\hat{F}$, assuming that H_0 is true. If the p-value is less than α (a typical threshold selection is 5%), H_0 is rejected. These concepts are sketched in Figure 7.

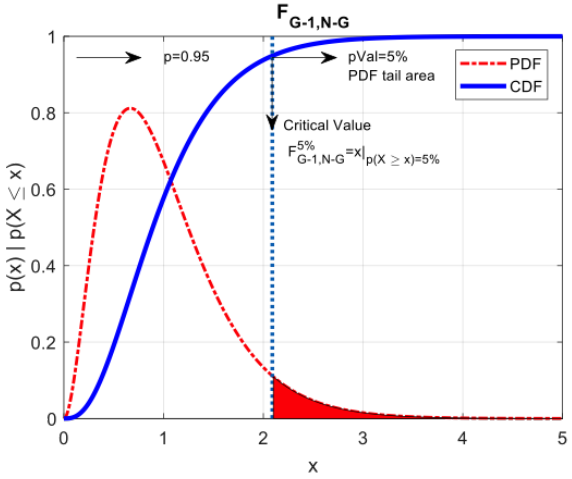


Figure 7. $F(G-1, N-G)$ distribution, with highlighted the 5% critical value and the concept of p-value.

For this analysis, the data sets are divided into two groups: the former one contains the healthy samples (TS1–TS9), and the latter one includes the features extracted from the time series of the damaged wind turbine (TS10–18).

The assumption of normality can be considered verified with enough confidence. The same does not hold for the homoscedasticity (equal variance in the different groups), but the ANOVA method is robust to these kinds of possible violations, and therefore the reliability of the results of this study is not affected. In the test case of this study, where only two groups are used, the ANOVA reduces to a

Student's *t*-test. The ANOVA is a univariate method and therefore it will repeated for each channel and feature combination (10 times): this in particular can give meaningful indications about the most powerful statistical indicators for damage detection.

3.4.2. Principal Component Analysis

The Principal Component Analysis (PCA) is a technique widely used in multivariate statistics [36], in particular for visualizing multi-dimensional data sets characterized by remarkable collinearity. In fact, the PCA is a space rotation to convert a set of correlated quantities into orthogonal variables called principal components: the first principal component explains the largest variance of the data set and each succeeding component explains the largest variance under the constraint of orthogonality with the preceding ones.

Let $\boldsymbol{X}_{n,p}$ be the matrix of observations: p is the number of columns, given in this study by the product of the number of channels times the number of features; n is the number of rows, i.e., the number of independent chunks of which the data set of interest is constituted. The principal component transformation can easily be expressed in terms of the singular value decomposition. Therefore, let

$$\boldsymbol{X} = \boldsymbol{U}\boldsymbol{\Delta}\boldsymbol{V}^T \tag{16}$$

be the singular value decomposition of $\boldsymbol{X}$. This means that the columns of $\boldsymbol{U}$ and $\boldsymbol{V}$ are orthonormal sets of vectors denoting the left and right singular vectors of $\boldsymbol{X}$ and $\boldsymbol{\Delta}$ is a diagonal matrix, whose elements are the singular values of $\boldsymbol{X}$. This allows for eigen-decompose $\boldsymbol{X}\boldsymbol{X}^T$ as:

$$\boldsymbol{X}\boldsymbol{X}^T = V\Lambda V^T, \tag{17}$$

where $\Lambda = diag\left(\lambda_1, \ldots, \lambda_p\right)$ and $\lambda_1 \geq \cdots \geq \lambda_p \geq 0$.

$\boldsymbol{X}\boldsymbol{V}_i$ is the i-th principal component and $\boldsymbol{V}_i$ is the i-th loading corresponding to the i-th principal value λ_i. The usefulness of the principal component analysis is that the decomposition in Equation (17) indicates a sort of regularization scheme: namely, the matrix $\boldsymbol{W}$ can be truncated including a desired number of principal components.

The Principal Component Analysis is employed in this study as for qualitative visualization of the data set by a more explanatory point of view, resulting from the space transform.

3.4.3. Novelty Index

In statistics, the anomaly identification can be performed point by point, studying how discordant each sample is with respect to the data set. A data point is commonly defined "outlier" when it can be considered statistically inconsistent with the others: a typical method for identifying outliers is detecting what measurements have a discrepancy with respect to the data set average that is higher than three data set standard deviations (the so-called 3σ rule). The judgment on data discordance with respect to a distribution can be performed also by analyzing an appropriately defined metric (i.e., a distance) of the data point of interest with respect to the data distribution: this provides a Novelty Index (NI) on which a threshold can be defined [37] for qualifying what points are statistically anomalous. The Mahalanobis distance is the optimal candidate for evaluating discordance in a multi-dimensional space because it is non-dimensional and scale-invariant, and takes into account the correlations of the data set. The Mahalanobis distance between one measurement z (possibly multi-dimensional) and the $\boldsymbol{X}$ distribution, whose covariance matrix is $\boldsymbol{S}$, is given by

$$MD = \sqrt{\left(z - \bar{\boldsymbol{X}}\right) \boldsymbol{S}^{-1} \left(z - \bar{\boldsymbol{X}}\right)}. \tag{18}$$

The Mahalanobis distance can be interpreted as a Euclidean distance in the feature space subjected to principal component transformation and standardization. In this study, the threshold for novelty detection is generated through several repeated Monte Carlo (MC) simulations of a 10-dimensional

Gaussian distribution. Drawing 240 observations (equal to the numerousness of the healthy reference set) and computing the NIs, the maximum value could be used to generate a robust threshold—for example, taking the 99th percentile of the maxima distribution [37].

The computation of the Mahalanobis Novelty Indices trained on healthy, normal condition data was selected for its intrinsic ability of compensating for linear and quasilinear confounding influences (i.e., environmental or operational variability) and for its robustness to noise [32,38]. In fact, training the algorithm corresponds to fitting a statistical model to the reference data (i.e., healthy, normal condition data): if the training data set covers the whole range of normal variability, any outlier can be then attributed to a non-normal condition.

For the purposes of this work, the reference $\boldsymbol{X}$ distribution is selected as the statistical features matrix extracted from the calibration data set of Table 1 (TS1–3). The target z is selected as the statistical features matrix extracted from the target data set of interest in Table 1. For example, computing the Mahalanobis distance, according to Equation (10), for each feature's observation in TS4–18, will be possible to appreciate the different statistical novelty of the target (healthy, damaged, and repaired) wind turbines with respect to the reference healthy ones.

4. Results

As explained in detail in Sections 3.1–3.3, the raw accelerometric signal has been pre-processed to remove the non-physical trends; subsequently, it has been divided in 100 chunks on which features (i.e., statistics of the signal) have been computed and, finally, the overall dataset of 1800 observations of 10 features each (five for the x-accelerations and five for the y-accelerations) has been cleaned of the anomalous observations referred to the machine adaptation to the changes in the work condition (i.e., mainly wind direction and speed). Finally, 1520 observations have been left, almost fairly divided into a healthy group of 756 points (from TS 1 to 9, considering also the repaired turbine as healthy) and a damaged group of 754 points (from TS 10 to 18).

The extracted features are shown in Figure 8 for the clean data set. The features extracted from the time series of the damaged wind turbines are placed in the subfigures on the right of the black dash-dot lines. From Figure 8, therefore, a powerful bird's eye view is obtained based on the fact that the damaged wind turbines are distinguishable with respect to the healthy wind turbines.

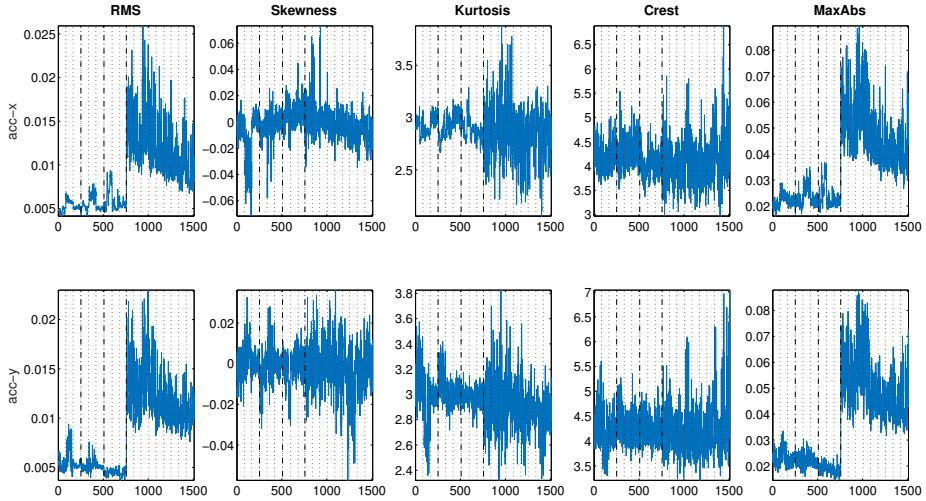


Figure 8. The statistical features computed on the cleaned data set. The different acquisitions are separated by the black dotted lines and ordered according to their corresponding TS number (Table 1). The healthy calibration data are separated from the healthy validation data, from the repaired validation data and from the damaged validation data by the black dash-dot lines.

Once the final data set is set up, the ANOVA is performed to test if diagnostic information is present in the different features: that is, if significant differences can be found between the healthy turbines observations (TS 1 to 9) and the damaged turbines observations (TS 10 to 18). As described in Section 3.4, the ANOVA outputs p-values corresponding to the probability that the null-hypothesis (i.e., no difference between the groups) is true. When the p-value is lower than 0.05, then the differences between the healthy and the damaged observations prove to be high enough to be detected, so that an effective diagnostic can be accomplished. Considering the cleaned data set, the resulting p-values are reported in Table 2.

As it can be easily seen, all the features prove to be clearly good for detecting the damage, except the Crest Factor of the accelerations from y-direction channel.

Table 2. The ANOVA p-values considering two groups: Healthy (TS1 to 9) vs Damaged (TS10 to 18).

Channel	RMS	Skewness	Kurtosis	Crest Factor	Peak
1 (X-dir)	0	0.28	1.4×10^{-14}	8.2×10^{-7}	0
2 (Y-dir)	0	9.4×10^{-7}	1.9×10^{-35}	0.59	0

The multivariate data set has then been visualized via PCA. The cleaned data set, rotated to match the principal directions, is reported in Figure 9: for readability of the Figure, it has been selected to report two-dimensional plots including up to the fourth principal component. It can be noticed that the dispersion of the damaged cloud (in red) is much larger, so that the red observations (in particular on the P2–P3 and P3–P4 planes) result in being more scattered and distinguishable.

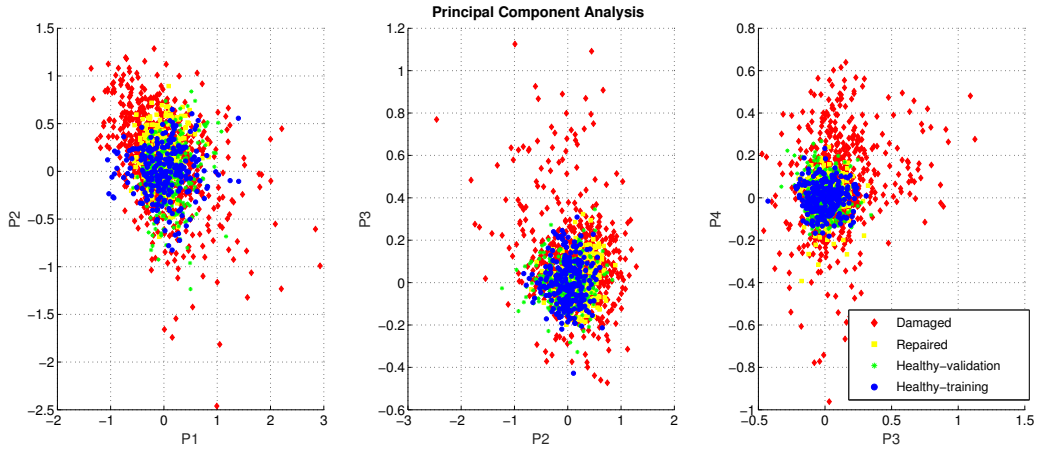


Figure 9. The data set projected on principal planes computed via PCA.

Computing the MD of all the observations from the centroid of the healthy reference distribution, the Novelty Indices shown in Figure 10 were obtained. The Monte Carlo threshold is drawn in red. According to such a threshold, the performance of the MD-NI damage detection is reported in Table 3 in terms of false and missed alarms. From the table, it is possible to understand that the algorithm is very good in discerning damaged from healthy acquisitions. it should be noticed that the repaired turbine data seems to show some differences with respect to the original healthy data. Using the same healthy reference for the repaired WTG06, then, could be not optimal.

The results in Figure 10 can be interpreted in light of the information reported in Table 1, in order to support the fact that the method is capable of correctly highlighting the faulty signatures. The acquisitions have been performed in couples: for each acquisition at a given time at the damaged wind turbine, there is a contemporary acquisition at a healthy wind turbine. TS4, 5, and 6 are contemporary

to, respectively, TS14, 16, and 18. The NI for each of TS4, 5, and 6 is coherently below the statistical threshold and the NI for each of the contemporary TS14, 16, and 18 is coherently well above the statistical threshold. This supports that the method is robust to detect as novelty the fault and not the different response of the wind turbines due to the wind field difference in space along the wind farm. Furthermore, consider two TS couples: (TS1, TS13) and (TS4, TS14). The first of each couple is a TS from a healthy wind turbine (WTG02) and the second is from the damaged wind turbine (WTG03); the two time series of each couple are acquired simultaneously. The operation conditions measured at the two wind turbines of the first TS pair are remarkably similar: the difference in generator speed average is less than 1.7%. For the second TS pair, the difference in generator speed average is more than 10%. From Figure 10, the statistical difference between TS1 and TS13 is indistinguishable with respect to the difference between TS4 and TS14. This supports that the novelty detection between the TS of WTG03 and the TS of the healthy wind turbines is indeed due to the damage and not due to slightly different operation conditions.

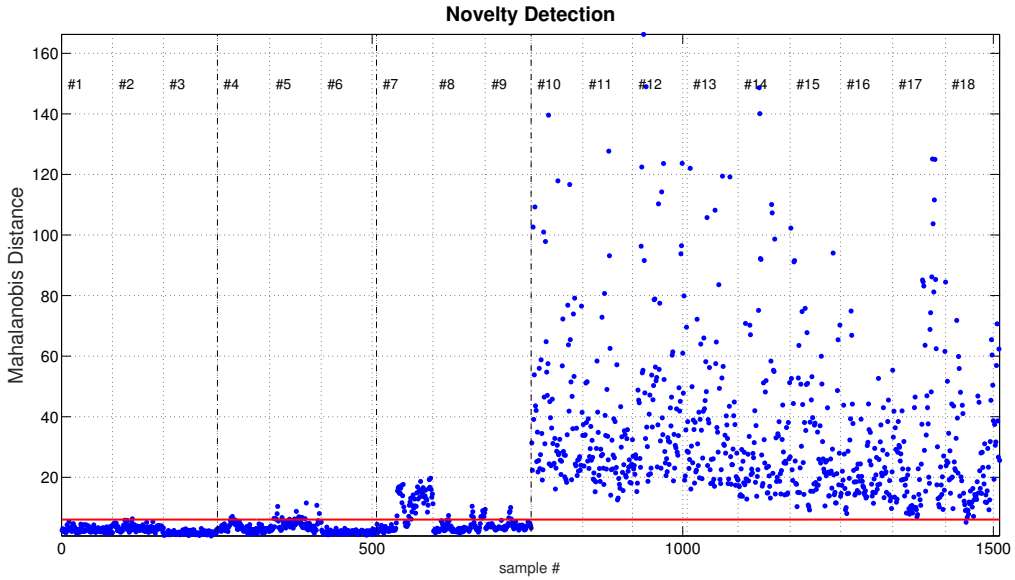


Figure 10. The Novelty Indices computed via Mahalanobis Distance. The MC threshold is visualized in red. The different acquisitions are separated by the black dotted lines and ordered according to their corresponding TS number. The healthy calibration data are separated from the healthy validation data, from the repaired validation data and from the damaged validation data by the black dash-dot lines.

Table 3. The MD-NI damage detection performance: False Alarms (FA) and Missed Alarms (MA).

	FA-Reference (TS1–3)	FA-Validation (TS4–6)	FA-Repaired (TS7–9)	MA-Damaged (TS10–18)
Alarms	0.4%	7.8%	28.5%	0.1%

5. Conclusions

A novel approach for damage detection at the drive-train subcomponents of wind turbine gearboxes has been proposed in this paper. The general idea is to measure the vibrations at the tower instead that at the gearbox, usually located in the nacelle in a hardly accessible area. This translates into simpler and less expensive acquisitions, whose reliability and effectiveness for damage detection is investigated in this work through a test case discussion.

The case study considered in this work deals with a high-speed shaft bearing damage at a wind turbine sited in Italy, owned and managed by the Renvico wind farm. The study consisted in on-site measurements and data post-processing.

The rationale for the measurements acquisition is exploiting the fact that wind turbines are typically grouped in clusters of nearby wind turbines, which, at a given time, should be subjected to reasonably similar solicitations: the expectation is that, if a wind turbine is damaged, it should have such a different response that it should be possible to distinguish it statistically with respect to healthy reference wind turbines, and the novelty identification should be possible also analyzing measurements collected at the tower.

For this study, therefore, tower accelerations have been measured at the target damaged wind turbine, at three healthy reference wind turbines and at a recently repaired wind turbine. This latter wind turbine has been included as a further contribution to the discussion because it is interesting to ask if it is distinguishable with respect to the healthy wind turbines.

In order to test the appropriateness of the measurements, a statistical analysis has been conducted on the post-processed and cleaned acceleration signals from which common time domain features such as RMS, Skewness, Kurtosis, Crest factor and Peak value have been extracted. The analysis started with the ANOVA, to test if a difference was detectable among the healthy and the damaged turbines acquisitions feature-wise (i.e., univariately). Then, the PCA was performed to visualize the data set projected on the first principal planes. Both techniques proved the detectability of the damage using the selected features extracted from the pre-processed tower acceleration measurements. Finally, the Mahalanobis Distance Novelty Detection showed optimal results in damage detection, given the low number of missed and false alarms. Another interesting result is that the repaired turbine resulted in being non-comparable to the healthy wind turbines because of an augmented value of false alarms.

In general, the algorithm proved to be an excellent damage detection routine, considering the quickness, the simplicity and the full independence from human interaction, which makes it suitable for real time implementations. This definitely motivates further research, also in light of the fact that the measurement procedure does not request altering the normal operation of the wind turbine and does not involve industrial plants security issues. This could foster the integration of vibration monitoring in the maintenance regimes of wind turbines, ensuring to the wind farms of the future higher reliability and minimal down times.

Another important development of this research is empowering the experimental techniques, in order to have reliable and high-frequency rotor angular speed measurements: this direction is currently being explored through video-tachometer [39] because it preserves the zero-impact philosophy of the approach. The availability of this kind of information, as well as of the gearbox geometry, is decisive for obtaining a precise identification of the damage location. Another line of further research regards the identification of the transfer functions of the machines: this development and the improvement of the experimental techniques would allow a more sophisticated signal processing and fault analysis, evolving with respect to the black box method of the present work.

Author Contributions: Conceptualization, D.A., F.C., A.P.D., F.N., and L.G. ; Data curation, F.C., A.P.D., and F.N.; Formal analysis, D.A., F.C., A.P.D., and L.G.; Investigation, D.A., F.C., A.P.D., F.N., and L.G; Methodology, F.C:, A.P.D., and L.G.; Project administration, F.C. and L.G.; Software, A.P.D. and F.N.; Supervision, F.C. and L.G., Validation, D.A., F.C., A.P.D., F.N., and L.G.; Writing—original draft, D.A. and A.P.D.; Writing—review and editing, F.C. and L.G. All authors have read and approved the final version of the manuscript

Funding: The authors acknowledge Fondazione "Cassa di Risparmio di Perugia" for the funded research project WIND4EV (WIND turbine technology EVolution for lifecycle optimization) and the Basic Research Plan 2018 of the Department of Engineering of the University of Perugia, for a financed project entitled "Investigation of the relations between surface micro-topography and vibration phenomena for couplings subjected to wear".

Acknowledgments: The authors would like to thank Ludovico Terzi, technology manager of the Renvico company.

Conflicts of Interest: The authors declare no conflict of interest.

Abbreviations

List of the abbreviations employed in the analysis.

Acronym	Meaning
ANOVA	Univariate Analysis of Variance
CREST	Crest Factor
E	Expectation value
FA	False alarms
KURT	Kurtosis
MA	Missing alarms
MAD	Median absolute deviation
MC	Monte Carlo
MD	Mahalanobis Distance
NI	Novelty Index
PCA	Principal Component Analysis
PEAK	Peak
RD	Robust Mahalanobis Distance
RMS	Root Mean Square
SKEW	Skewness

References

1. Rafiee, J.; Arvani, F.; Harifi, A.; Sadeghi, M. Intelligent condition monitoring of a gearbox using artificial neural network. *Mech. Syst. Signal Process.* **2007**, *21*, 1746–1754.
2. Smolders, K.; Long, H.; Feng, Y.; Tavner, P. Reliability analysis and prediction of wind turbine gearboxes. In Proceedings of the European Wind Energy Conference and Exhibition 2010, EWEC 2010, Warsaw, Poland, 20–23 April 2010; Volume 4, pp. 2660–2682.
3. Bhardwaj, U.; Teixeira, A.; Soares, C.G. Reliability prediction of an offshore wind turbine gearbox. *Renew. Energy* **2019**, *141*, 693–706.
4. Carroll, J.; McDonald, A.; McMillan, D. Failure rate, repair time and unscheduled O&M cost analysis of offshore wind turbines. *Wind Energy* **2016**, *19*, 1107–1119.
5. Tchakoua, P.; Wamkeue, R.; Ouhrouche, M.; Slaoui-Hasnaoui, F.; Tameghe, T.A.; Ekemb, G. Wind turbine condition monitoring: State-of-the-art review, new trends, and future challenges. *Energies* **2014**, *7*, 2595–2630.
6. López de Calle, K.; Ferreiro, S.; Roldán-Paraponiaris, C.; Ulazia, A. A Context-Aware Oil Debris-Based Health Indicator for Wind Turbine Gearbox Condition Monitoring. *Energies* **2019**, *12*, 3373.
7. Wang, Y.; Infield, D. Supervisory control and data acquisition data-based nonlinear state estimation technique for wind turbine gearbox condition monitoring. *IET Renew. Power Gener.* **2013**, *7*, 350–358.
8. Astolfi, D.; Castellani, F.; Terzi, L. Fault prevention and diagnosis through scada temperature data analysis of an onshore wind farm. *Diagnostyka* **2014**, *15*, 71–78.
9. Sequeira, C.; Pacheco, A.; Galego, P.; Gorbeña, E. Analysis of the efficiency of wind turbine gearboxes using the temperature variable. *Renew. Energy* **2019**, *135*, 465–472.
10. Guo, P.; Fu, J.; Yang, X. Condition Monitoring and Fault Diagnosis of Wind Turbines Gearbox Bearing Temperature Based on Kolmogorov–Smirnov Test and Convolutional Neural Network Model. *Energies* **2018**, *11*, 2248.
11. Qian, P.; Tian, X.; Kanfoud, J.; Lee, J.L.Y.; Gan, T.H. A novel condition monitoring method of wind turbines based on long short-term memory neural network. *Energies* **2019**, *12*, 3411.
12. Carroll, J.; Koukoura, S.; McDonald, A.; Charalambous, A.; Weiss, S.; McArthur, S. Wind turbine gearbox failure and remaining useful life prediction using machine learning techniques. *Wind Energy* **2019**, *22*, 360–375.
13. Zhang, Z.; Verma, A.; Kusiak, A. Fault analysis and condition monitoring of the wind turbine gearbox. *IEEE Trans. Energy Convers.* **2012**, *27*, 526–535.
14. Igba, J.; Alemzadeh, K.; Durugbo, C.; Eiriksson, E.T. Analysing RMS and peak values of vibration signals for condition monitoring of wind turbine gearboxes. *Renew. Energy* **2016**, *91*, 90–106.
15. Peeters, C.; Guillaume, P.; Helsen, J. Vibration-based bearing fault detection for operations and maintenance cost reduction in wind energy. *Renew. Energy* **2018**, *116*, 74–87.
16. Antoni, J. Cyclic spectral analysis in practice. *Mech. Syst. Signal Process.* **2007**, *21*, 597–630.

17. Antoniadou, I.; Manson, G.; Staszewski, W.; Barszcz, T.; Worden, K. A time-frequency analysis approach for condition monitoring of a wind turbine gearbox under varying load conditions. *Mech. Syst. Signal Process.* **2015**, *64*, 188–216.
18. Shi, P.; Yang, W.; Sheng, M.; Wang, M. An enhanced empirical wavelet transform for features extraction from wind turbine condition monitoring signals. *Energies* **2017**, *10*, 972.
19. Feng, Z.; Chen, X.; Liang, M. Iterative generalized synchrosqueezing transform for fault diagnosis of wind turbine planetary gearbox under nonstationary conditions. *Mech. Syst. Signal Process.* **2015**, *52*, 360–375.
20. Hossain, M.; Abu-Siada, A.; Muyeen, S. Methods for advanced wind turbine condition monitoring and early diagnosis: A literature review. *Energies* **2018**, *11*, 1309.
21. Wang, T.; Han, Q.; Chu, F.; Feng, Z. Vibration based condition monitoring and fault diagnosis of wind turbine planetary gearbox: A review. *Mech. Syst. Signal Process.* **2019**, *126*, 662–685.
22. Castellani, F.; Sdringola, P.; Astolfi, D. Analysis of wind turbine wakes through time-resolved and SCADA data of an onshore wind farm. *J. Sol. Energy Eng.* **2018**, *140*, 044501.
23. Gonzalez, E.; Stephen, B.; Infield, D.; Melero, J.J. Using high-frequency SCADA data for wind turbine performance monitoring: A sensitivity study. *Renew. Energy* **2019**, *131*, 841–853.
24. Wang, X.; Yan, X.; He, Y. Weak Fault Feature Extraction and Enhancement of Wind Turbine Bearing Based on OCYCBD and SVDD. *Appl. Sci.* **2019**, *9*, 3706.
25. Mollasalehi, E.; Wood, D.; Sun, Q. Indicative fault diagnosis of wind turbine generator bearings using tower sound and vibration. *Energies* **2017**, *10*, 1853.
26. Elforjani, M.; Bechhoefer, E. Analysis of extremely modulated faulty wind turbine data using spectral kurtosis and signal intensity estimator. *Renew. Energy* **2018**, *127*, 258–268.
27. Elforjani, M.; Shanbr, S.; Bechhoefer, E. Detection of faulty high speed wind turbine bearing using signal intensity estimator technique. *Wind Energy* **2018**, *21*, 53–69.
28. Elforjani, M. Diagnosis and prognosis of real world wind turbine gears. *Renew. Energy* **2020**, *147*, 1676–1693.
29. Smith, S.W. *The Scientist and Engineer's Guide to Digital Signal Processing*; California Technical Pub: Pasadena, CA, USA, 1997.
30. Liu, H.; Shah, S.; Jiang, W. On-line outlier detection and data cleaning. *Comput. Chem. Eng.* **2004**, *28*, 1635–1647.
31. Pearson, R.K.; Neuvo, Y.; Astola, J.; Gabbouj, M. The class of generalized hampel filters. In Proceedings of the IEEE 23rd European Signal Processing Conference (EUSIPCO), Nice, France, 31 August–4 September 2015; pp. 2501–2505.
32. Daga, A.P.; Garibaldi, L. Machine Vibration Monitoring for Diagnostics through Hypothesis Testing. *Information* **2019**, *10*, 204.
33. Daga, A.P.; Fasana, A.; Marchesiello, S.; Garibaldi, L. The Politecnico di Torino rolling bearing test rig: Description and analysis of open access data. *Mech. Syst. Signal Process.* **2019**, *120*, 252–273.
34. Hubert, M.; Debruyne, M. Minimum covariance determinant. In *Wiley Interdisciplinary Reviews: Computational Statistics*; Wiley: Hoboken, NJ, USA, 2010; Volume 2, pp. 36–43.
35. Sahai, H.; Ageel, M.I. *The Analysis of Variance: Fixed, Random and Mixed Models*; Springer Science & Business Media: Berlin, Germany, 2012.
36. Abdi, H.; Williams, L.J. Principal component analysis. In *Wiley Interdisciplinary Reviews: Computational Statistics*; Wiley: Hoboken, NJ, USA 2010; Volume 2, pp. 433–459.
37. Worden, K.; Manson, G.; Fieller, N.R. Damage detection using outlier analysis. *J. Sound Vib.* **2000**, *229*, 647–667.
38. Deraemaeker, A.; Worden, K. A comparison of linear approaches to filter out environmental effects in structural health monitoring. *Mech. Syst. Signal Process.* **2018**, *105*, 1–15.
39. Daga, A.P.; Garibaldi, L. GA-Adaptive Template Matching for Offline Shape Motion Tracking Based on Edge Detection: IAS Estimation from the SURVISHNO 2019 Challenge Video for Machine Diagnostics Purposes. *Algorithms* **2020**, *13*, 33.



© 2020 by the authors. Licensee MDPI, Basel, Switzerland. This article is an open access article distributed under the terms and conditions of the Creative Commons Attribution (CC BY) license (http://creativecommons.org/licenses/by/4.0/).